# FORECASTERS' FORUM

# The Challenge of Forecasting Significant Tornadoes from June to October Using Convective Parameters

JOHN A. HART AND ARIEL E. COHEN

*NOAA/NWS/NCEP/Storm Prediction Center, Norman, Oklahoma*

(Manuscript received 29 December 2015, in final form 9 August 2016)

## ABSTRACT

This study is an application of the Statistical Severe Convective Risk Assessment Model (SSCRAM), which objectively assesses conditional severe thunderstorm probabilities based on archived hourly mesoscale data across the United States collected from 2006 to 2014. In the present study, SSCRAM is used to assess the utility of severe thunderstorm parameters commonly employed by forecasters in anticipating thunderstorms that produce significant tornadoes (i.e., causing F2/EF2 or greater damage) from June through October. The utility during June–October is compared to that during other months. Previous studies have identified some aspects of the summertime challenge in severe storm forecasting, and this study provides an in-depth quantification of the within-year variability of severe storms predictability. Conditional probabilities of significant tornadoes downstream of lightning occurrence using common parameter values, such as the effective-layer significant tornado parameter, convective available potential energy, and vertical shear, are found to substantially decrease during the months of June–October compared to other months. Furthermore, conditional probabilities of significant tornadoes during June–October associated with these parameters are nearly invariable regardless of value, highlighting the challenge of using objective environmental data to attempt to forecast significant tornadoes from June through October.

## 1. Introduction

Attempts to improve tornado forecasting extend throughout a large part of the twentieth century to the present day owing to the high-impact nature of such phenomena. An awareness of the meteorological environment with respect to assessing severe thunderstorm potential is a fundamental component of forecasting tornadoes. In fact, the notion of assessing the meteorological environment in proximity to a tornadic storm can be traced to the 1960s and 1970s (e.g., Darkow 1968, 1969) through the use of environmental soundings. The approach to evaluating severe thunderstorm potential has evolved to anticipating the potential for mutual spatiotemporal overlap of kinematic and thermodynamic necessary conditions (e.g., Doswell 1987; Johns and Doswell 1992). The intra-annual variability of tornado potential associated with kinematic and thermodynamic parameters to assess these necessary conditions is the focus of this work.

Through the early years of research regarding the environments of severe storms including tornadoes, tornado-favoring environments are characterized by relatively larger magnitudes of buoyancy [vertically integrated to yield convective available potential energy (CAPE)] and vertical shear (e.g., Rasmussen and Wilhelmson 1983), in the most general terms. In recent years, a multitude of individual and composite parameters has been developed and tested to further categorize and discriminate among severe weather environments; these parameters are used to evaluate the ingredients relevant for severe storm forecasting. Each is a unique, statistically derived combination of parameters that can be determined from soundings based upon the phenomenon that it attempts to identify and/or forecast. For example, for deep, moist convection, Craven and Brooks (2004) evaluated the forecast utility of numerous parameters in anticipating the potential presence and severity of thunderstorms. With respect to environments supporting tornadic storms, the energy–helicity index (EHI; Hart and Korotky 1991) is an example of a parameter used to diagnose tornado potential. Even more

---

*Corresponding author address*: John Hart, Storm Prediction Center, 120 David L. Boren Blvd., Norman, OK 73072.
E-mail: john.hart@noaa.gov

DOI: 10.1175/WAF-D-16-0005.1

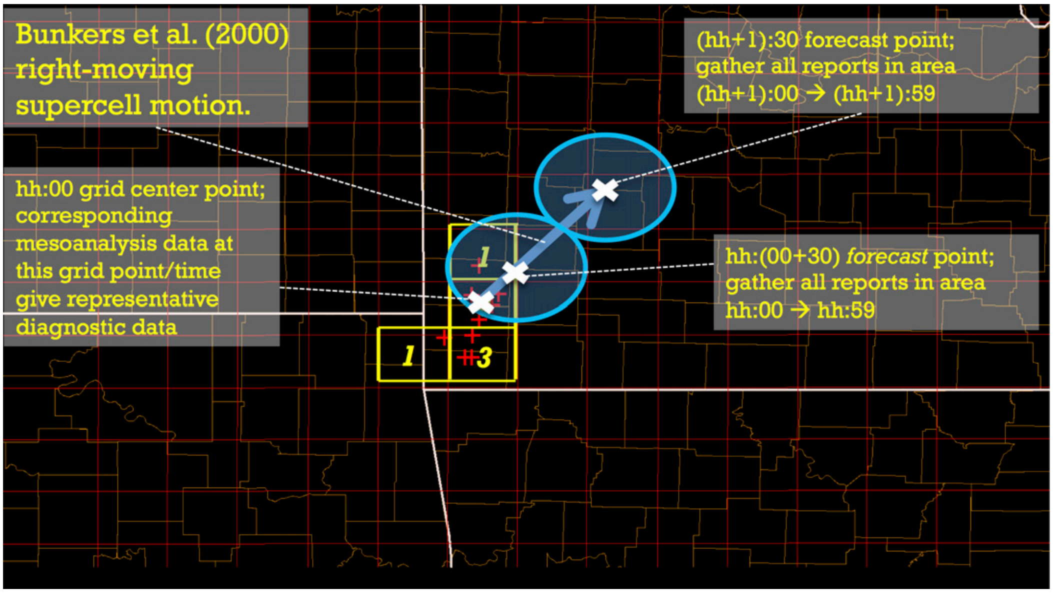

FIG. 1. Schematic that demonstrates the process of ascertaining downstream severe storm reports from each lightning-associated grid box. This figure illustrates two different search zones centered on two respective points extrapolated forward in space from the lightning-associated grid center point, based upon the Bunkers et al.'s (2000) right-moving supercell motion technique. Search circles centered along the projected storm path extend outward to 40 km. This represents a cumulative total of 2 h of severe storm report collection forward in time from the lightning-associated grid box. Severe reports in each search circle are restricted to those occurring within 30 min of the time corresponding to each respective forward-extrapolated point. [Reproduced from Hart and Cohen (2016).]

recently, Thompson et al. (2012) demonstrated the utility of the effective-layer significant tornado parameter (STP) in identifying environments that support significant tornadoes (i.e., producing F2/EF2 damage).

Many of the aforementioned parameters, particularly ones involving forms of CAPE, vertical shear, and combinations of these, have become well instilled within the vernacular of the modern-day severe thunderstorm forecaster. Their values are associated with often-cited numerical benchmarks that are used as guidance in characterizing the propensity of particular environments to support severe thunderstorms. Given the diagnostic nature of these variables, their use as forecasting proxies is questionable, at best. Specifically, Doswell and Schultz (2006) deemed diagnostic parameters describing initial atmospheric conditions as having limited predictability of the future state of the atmosphere. However, they did identify the possibility of using diagnostic data to explicitly express probabilistic information in severe thunderstorm forecasting, in which the combination of occurrences of events and nonevents (null cases) is used to derive the probability of event occurrence. This notion is the foundation of a companion paper, in which Hart and Cohen (2016) developed the Statistical Severe Convective Risk Assessment Model (SSCRAM). This system couples 9 yr of lightning data to severe thunderstorm reports to evaluate 1) the conditional probability of severe thunderstorm reports occurring downstream of observed lightning occurrences and 2) the relative frequency of severe thunderstorm reports occurring within various ranges of numerous parameters.

SSCRAM systematically addresses the predictability of diagnostic parameters as motivated by Doswell and Schultz (2006), and Hart and Cohen (2016) provided examples of the relationship between a subset of five thermodynamic, kinematic, and composite variables in forecasting individual severe storm hazards (wind, hail, and tornadoes). Relevant to the present study, they provided a specific focus on parameters associated with tornado forecasting, and identified conditional tornado probabilities given lightning occurrence. These probabilities show that effective-layer STP and effective storm-relative helicity provide the greatest utility in forecasting significant tornadoes (i.e., an increase in parameter values is often related to an increase in the probability of occurrence). On the other hand, individual thermodynamic parameters such as lifting condensation level (LCL) height and instability quantities yield substantially weaker forecast utility.

With SSCRAM having a large sample size, being built upon nearly 3.8 million data points, it affords us the opportunity to broaden the scope of severe storm probabilistic parameter-based guidance. This not only includes an

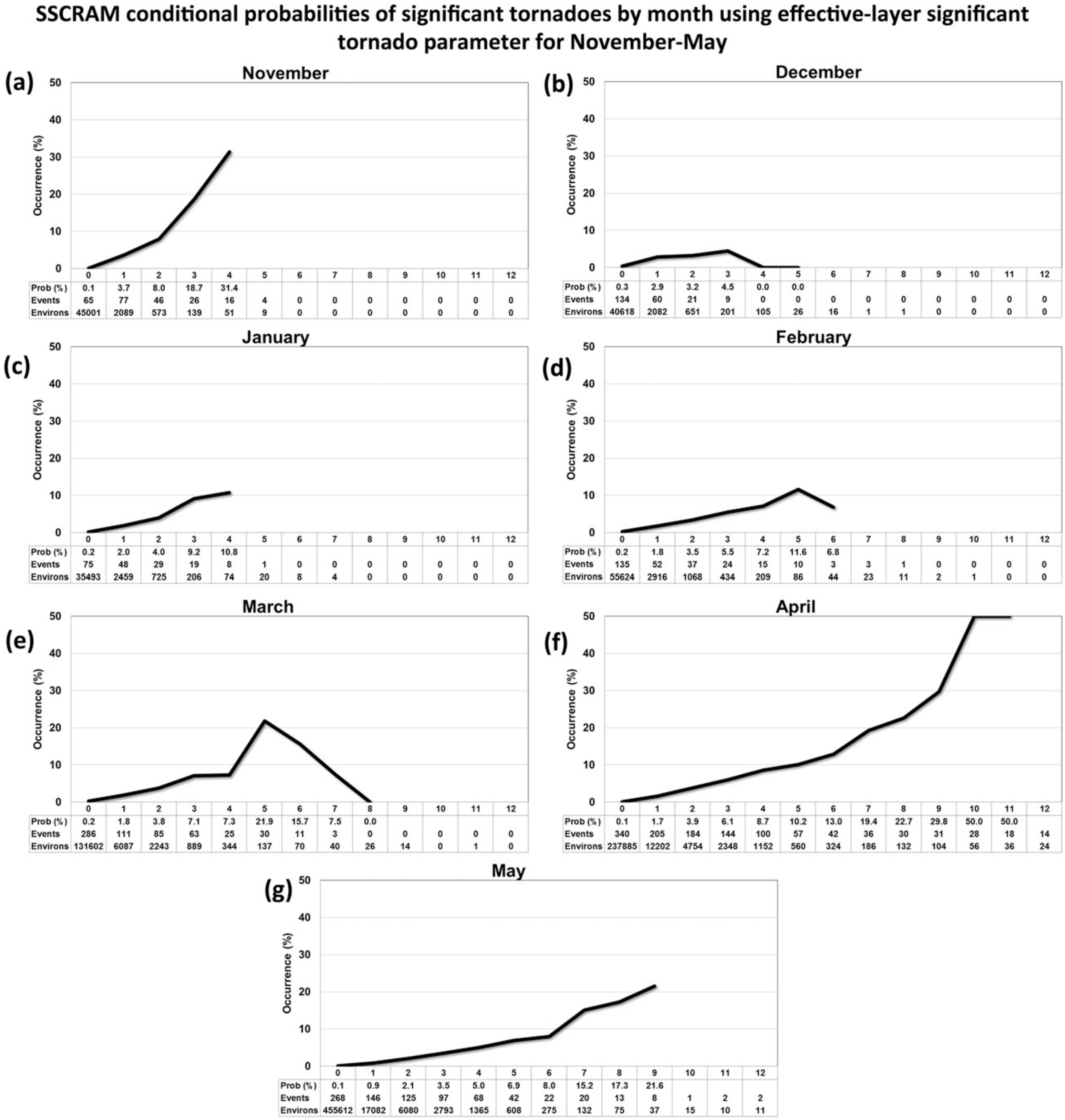

SSCRAM conditional probabilities of significant tornadoes by month using effective-layer significant tornado parameter for November-May

(a) November

| | 0 | 1 | 2 | 3 | 4 | 5 | 6 | 7 | 8 | 9 | 10 | 11 | 12 |
|---|---|---|---|---|---|---|---|---|---|---|---|---|---|
| Prob (%) | 0.1 | 3.7 | 8.0 | 18.7 | 31.4 | | | | | | | | |
| Events | 65 | 77 | 46 | 26 | 16 | 4 | 0 | 0 | 0 | 0 | 0 | 0 | 0 |
| Environs | 45001 | 2089 | 573 | 139 | 51 | 9 | 0 | 0 | 0 | 0 | 0 | 0 | 0 |

(b) December

| | 0 | 1 | 2 | 3 | 4 | 5 | 6 | 7 | 8 | 9 | 10 | 11 | 12 |
|---|---|---|---|---|---|---|---|---|---|---|---|---|---|
| Prob (%) | 0.3 | 2.9 | 3.2 | 4.5 | 0.0 | 0.0 | | | | | | | |
| Events | 134 | 60 | 21 | 9 | 0 | 0 | 0 | 0 | 0 | 0 | 0 | 0 | 0 |
| Environs | 40618 | 2082 | 651 | 201 | 105 | 26 | 16 | 1 | 1 | 0 | 0 | 0 | 0 |

(c) January

| | 0 | 1 | 2 | 3 | 4 | 5 | 6 | 7 | 8 | 9 | 10 | 11 | 12 |
|---|---|---|---|---|---|---|---|---|---|---|---|---|---|
| Prob (%) | 0.2 | 2.0 | 4.0 | 9.2 | 10.8 | | | | | | | | |
| Events | 75 | 48 | 29 | 19 | 8 | 1 | 0 | 0 | 0 | 0 | 0 | 0 | 0 |
| Environs | 35493 | 2459 | 725 | 206 | 74 | 20 | 8 | 4 | 0 | 0 | 0 | 0 | 0 |

(d) February

| | 0 | 1 | 2 | 3 | 4 | 5 | 6 | 7 | 8 | 9 | 10 | 11 | 12 |
|---|---|---|---|---|---|---|---|---|---|---|---|---|---|
| Prob (%) | 0.2 | 1.8 | 3.5 | 5.5 | 7.2 | 11.6 | 6.8 | | | | | | |
| Events | 135 | 52 | 37 | 24 | 15 | 10 | 3 | 3 | 1 | 0 | 0 | 0 | 0 |
| Environs | 55624 | 2916 | 1068 | 434 | 209 | 86 | 44 | 23 | 11 | 2 | 1 | 0 | 0 |

(e) March

| | 0 | 1 | 2 | 3 | 4 | 5 | 6 | 7 | 8 | 9 | 10 | 11 | 12 |
|---|---|---|---|---|---|---|---|---|---|---|---|---|---|
| Prob (%) | 0.2 | 1.8 | 3.8 | 7.1 | 7.3 | 21.9 | 15.7 | 7.5 | 0.0 | | | | |
| Events | 286 | 111 | 85 | 63 | 25 | 30 | 11 | 3 | 0 | 0 | 0 | 0 | 0 |
| Environs | 131602 | 6087 | 2243 | 889 | 344 | 137 | 70 | 40 | 26 | 14 | 0 | 1 | 0 |

(f) April

| | 0 | 1 | 2 | 3 | 4 | 5 | 6 | 7 | 8 | 9 | 10 | 11 | 12 |
|---|---|---|---|---|---|---|---|---|---|---|---|---|---|
| Prob (%) | 0.1 | 1.7 | 3.9 | 6.1 | 8.7 | 10.2 | 13.0 | 19.4 | 22.7 | 29.8 | 50.0 | 50.0 | |
| Events | 340 | 205 | 184 | 144 | 100 | 57 | 42 | 36 | 30 | 31 | 28 | 18 | 14 |
| Environs | 237885 | 12202 | 4754 | 2348 | 1152 | 560 | 324 | 186 | 132 | 104 | 56 | 36 | 24 |

(g) May

| | 0 | 1 | 2 | 3 | 4 | 5 | 6 | 7 | 8 | 9 | 10 | 11 | 12 |
|---|---|---|---|---|---|---|---|---|---|---|---|---|---|
| Prob (%) | 0.1 | 0.9 | 2.1 | 3.5 | 5.0 | 6.9 | 8.0 | 15.2 | 17.3 | 21.6 | | | |
| Events | 268 | 146 | 125 | 97 | 68 | 42 | 22 | 20 | 13 | 8 | 1 | 2 | 2 |
| Environs | 455612 | 17082 | 6080 | 2793 | 1365 | 608 | 275 | 132 | 75 | 37 | 15 | 10 | 11 |

FIG. 2. Conditional probabilities of significant tornadoes based on the effective-layer STP by month during N–M, with each month of the year corresponding to a panel labeled by the month's name. Conditional probabilities (Prob) are derived by dividing the number of grid boxes associated with reported downstream significant tornadoes (Events) by the number of grid boxes merely meeting constraints of lightning occurrence and STP range (Environs). Labels immediately beneath the $x$ axis provide the lower bounds of STP ranges and corresponding Prob, Events, and Environs values. The Prob values are not provided for parameter-bin ranges with Environs values < 25.

investigation of the probabilistic utility of various variables at large, but also includes an investigation of their *seasonal* utility. The stratification of the SSCRAM dataset based on tornado intensity *and* season builds upon work on tornado-related conditional probability evaluation developed by Togstad et al. (2011) and Smith et al. (2015) by adding a seasonal component. The purpose of the present study is to identify differences in the forecast utility associated with parameters describing tornado environments throughout the year.

While the physical laws governing severe storm development are invariable, the forecast utility of parameters

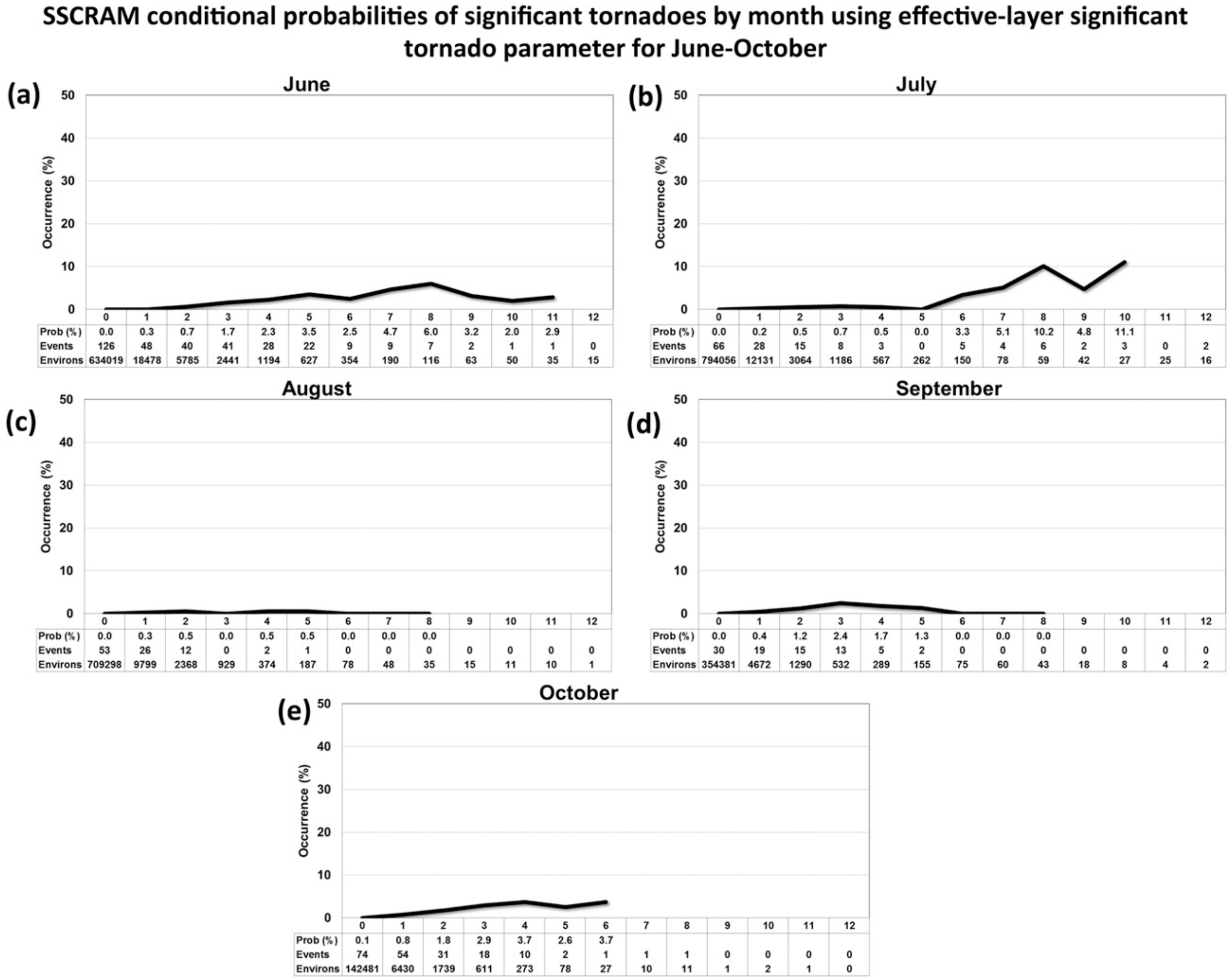

SSCRAM conditional probabilities of significant tornadoes by month using effective-layer significant tornado parameter for June-October

(a) June

| | 0 | 1 | 2 | 3 | 4 | 5 | 6 | 7 | 8 | 9 | 10 | 11 | 12 |
|---|---|---|---|---|---|---|---|---|---|---|---|---|---|
| Prob (%) | 0.0 | 0.3 | 0.7 | 1.7 | 2.3 | 3.5 | 2.5 | 4.7 | 6.0 | 3.2 | 2.0 | 2.9 | |
| Events | 126 | 48 | 40 | 41 | 28 | 22 | 9 | 9 | 7 | 2 | 1 | 1 | 0 |
| Environs | 634019 | 18478 | 5785 | 2441 | 1194 | 627 | 354 | 190 | 116 | 63 | 50 | 35 | 15 |

(b) July

| | 0 | 1 | 2 | 3 | 4 | 5 | 6 | 7 | 8 | 9 | 10 | 11 | 12 |
|---|---|---|---|---|---|---|---|---|---|---|---|---|---|
| Prob (%) | 0.0 | 0.2 | 0.5 | 0.7 | 0.5 | 0.0 | 3.3 | 5.1 | 10.2 | 4.8 | 11.1 | | |
| Events | 66 | 28 | 15 | 8 | 3 | 0 | 5 | 4 | 6 | 2 | 3 | 0 | 2 |
| Environs | 794056 | 12131 | 3064 | 1186 | 567 | 262 | 150 | 78 | 59 | 42 | 27 | 25 | 16 |

(c) August

| | 0 | 1 | 2 | 3 | 4 | 5 | 6 | 7 | 8 | 9 | 10 | 11 | 12 |
|---|---|---|---|---|---|---|---|---|---|---|---|---|---|
| Prob (%) | 0.0 | 0.3 | 0.5 | 0.0 | 0.5 | 0.5 | 0.0 | 0.0 | 0.0 | | | | |
| Events | 53 | 26 | 12 | 0 | 2 | 1 | 0 | 0 | 0 | 0 | 0 | 0 | 0 |
| Environs | 709298 | 9799 | 2368 | 929 | 374 | 187 | 78 | 48 | 35 | 15 | 11 | 10 | 1 |

(d) September

| | 0 | 1 | 2 | 3 | 4 | 5 | 6 | 7 | 8 | 9 | 10 | 11 | 12 |
|---|---|---|---|---|---|---|---|---|---|---|---|---|---|
| Prob (%) | 0.0 | 0.4 | 1.2 | 2.4 | 1.7 | 1.3 | 0.0 | 0.0 | 0.0 | | | | |
| Events | 30 | 19 | 15 | 13 | 5 | 2 | 0 | 0 | 0 | 0 | 0 | 0 | 0 |
| Environs | 354381 | 4672 | 1290 | 532 | 289 | 155 | 75 | 60 | 43 | 18 | 8 | 4 | 2 |

(e) October

| | 0 | 1 | 2 | 3 | 4 | 5 | 6 | 7 | 8 | 9 | 10 | 11 | 12 |
|---|---|---|---|---|---|---|---|---|---|---|---|---|---|
| Prob (%) | 0.1 | 0.8 | 1.8 | 2.9 | 3.7 | 2.6 | 3.7 | | | | | | |
| Events | 74 | 54 | 31 | 18 | 10 | 2 | 1 | 1 | 1 | 0 | 0 | 0 | 0 |
| Environs | 142481 | 6430 | 1739 | 611 | 273 | 78 | 27 | 10 | 11 | 1 | 2 | 1 | 0 |

FIG. 3. As in Fig. 2, but for the months of J–O.

that only partially represent these laws may certainly be variable, especially considering the wide array of convective modes that either support or inhibit tornadogenesis (e.g., Smith et al. 2012; Thompson et al. 2012; Edwards et al. 2012). More specifically, the relevance of a given parameter during one season in terms of anticipating downstream severe thunderstorm occurrence of observed lightning may not be the same in another season. Previous research has indeed highlighted the complexities of warm-season convective regimes. For example, Jankov and Gallus (2004) identified challenges in forecasting during weak-forcing-for-ascent convective regimes, which more frequently typify warm-season patterns, from a numerical modeling perspective. These findings highlight previous research that identifies aspects of warm-season severe storms forecasting that could prove to be challenging, particularly from a tornado-forecasting aspect.

Interseasonal variability for certain parameters in forecasting tornado potential may render all-season parameter-based severe storm probabilities less useful for individual seasons, along with other parameter-derived output for conditional tornado probabilities as identified by previous work, including Hart and Cohen (2016) and Togstad et al. (2011). Quantifying this variability in predictability for significant tornadoes using the SSCRAM system is the focus of the present work.

## 2. Data, methods, and analysis

SSCRAM, as described by Hart and Cohen (2016), is used as the basis for evaluating probabilities of severe storm occurrence given a lightning strike and mesoscale environmental information in proximity to the lightning. These probabilities correspond to severe storm occurrence downstream of the initial-hour grid box corresponding to the lightning strike(s), as illustrated in Fig. 1, with forward motion estimated from Bunkers et al.'s (2000) right-moving supercell motion technique. As

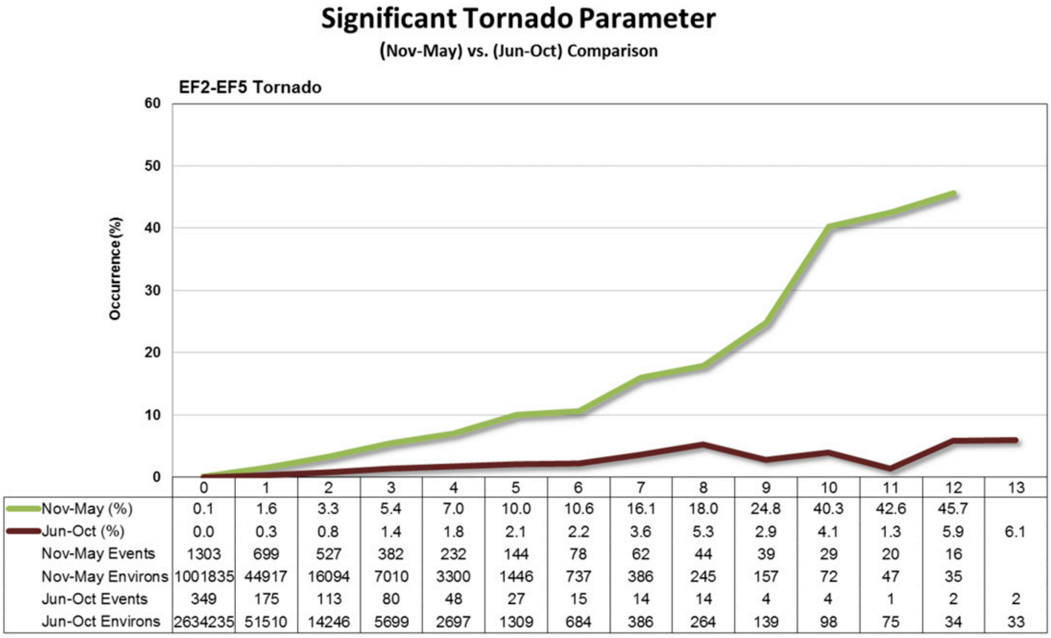

| | 0 | 1 | 2 | 3 | 4 | 5 | 6 | 7 | 8 | 9 | 10 | 11 | 12 | 13 |
|---|---|---|---|---|---|---|---|---|---|---|---|---|---|---|
| 🟩 Nov-May (%) | 0.1 | 1.6 | 3.3 | 5.4 | 7.0 | 10.0 | 10.6 | 16.1 | 18.0 | 24.8 | 40.3 | 42.6 | 45.7 | |
| 🟥 Jun-Oct (%) | 0.0 | 0.3 | 0.8 | 1.4 | 1.8 | 2.1 | 2.2 | 3.6 | 5.3 | 2.9 | 4.1 | 1.3 | 5.9 | 6.1 |
| Nov-May Events | 1303 | 699 | 527 | 382 | 232 | 144 | 78 | 62 | 44 | 39 | 29 | 20 | 16 | |
| Nov-May Environs | 1001835 | 44917 | 16094 | 7010 | 3300 | 1446 | 737 | 386 | 245 | 157 | 72 | 47 | 35 | |
| Jun-Oct Events | 349 | 175 | 113 | 80 | 48 | 27 | 15 | 14 | 14 | 4 | 4 | 1 | 2 | 2 |
| Jun-Oct Environs | 2634235 | 51510 | 14246 | 5699 | 2697 | 1309 | 684 | 386 | 264 | 139 | 98 | 75 | 34 | 33 |

FIG. 4. Conditional probabilities of significant tornadoes based on STP grouped from N–M (dark green) and overlaid with those grouped from J–O (dark brown). Corresponding values of conditional probabilities are listed beneath the $x$ axis, along with the number of grid boxes associated with the reported downstream significant tornadoes (Events) and the number of grid boxes merely meeting constraints (Environs) of lightning occurrence and STP range. Labels immediately beneath the $x$ axis provide the lower bounds of STP ranges. For each parameter-range bin, the conditional probability is equivalent to the Events value divided by the Environs value and is not computed for parameter-bin ranges with Environs values $< 25$.

described by Hart and Cohen (2016) regarding the development of the SSCRAM system, the Bunkers et al. (2000) technique seems to be an appropriate method for estimating storm motion for the purposes of this study when compared to other storm motion estimates, including the modified Bunkers et al. (2014) technique, the 30R75 method [i.e., estimate of storm motion direction to be to the right of the mean wind by 30°, with storm motion magnitude being 75% of the mean wind speed per Maddox (1976)], and the pressure-weighted mean wind. SSCRAM provides both the conditional probability of severe-event occurrence within particular ranges of parameter values, and the relative frequency of severe-event occurrences for various ranges of a parameter-value spectrum. The present study exhibits these concepts in subsequently described figures.

Hart and Cohen (2016) demonstrated the overall utility of STP in assessing tornado probabilities downstream of lightning-producing convection, with notably increasing significant tornado probability as STP increases. The STP combines effective storm-relative helicity (Thompson et al. 2007), the LCL of the lowest-100-mb mixed-layer parcel, effective bulk shear (Thompson et al. 2007), mixed-layer convective available potential energy (MLCAPE), and mixed-layer convective inhibition (MLCIN). Examination of the conditional probabilities of significant tornado occurrence reveals the variable utility of STP from month to month (Figs. 2 and 3). Specifically, there is a much stronger practical relationship between STP and significant tornado occurrences in April, compared to September when conditional probabilities vary little across STP values. This suggests less utility of STP in evaluating downstream significant tornado potential in September compared to April.

For the purposes of generalizing our results, we analyze temporally continuous periods of similar-characteristic significant tornado predictability. There appear to be two distinct periods during which the characteristics of the probability distributions in predicting significant tornadoes using STP are similar (Figs. 2 and 3). Specifically, months from November through May (N–M) are associated with general increases in conditional probabilities with increasing STP values. One exception is December, though the sample sizes of environments in December are relatively small, permitting its inclusion in the continuous N–M period. Other exceptions include small perturbations within the spectrum of STP values whose physical explanations are outside the scope of this work. Meanwhile, the months of June–October (J–O) are associated with little variability across STP values for these conditional probabilities. Subsequently, the

(a) 100mb Mixed-Layer CAPE (J $kg^{-1}$)

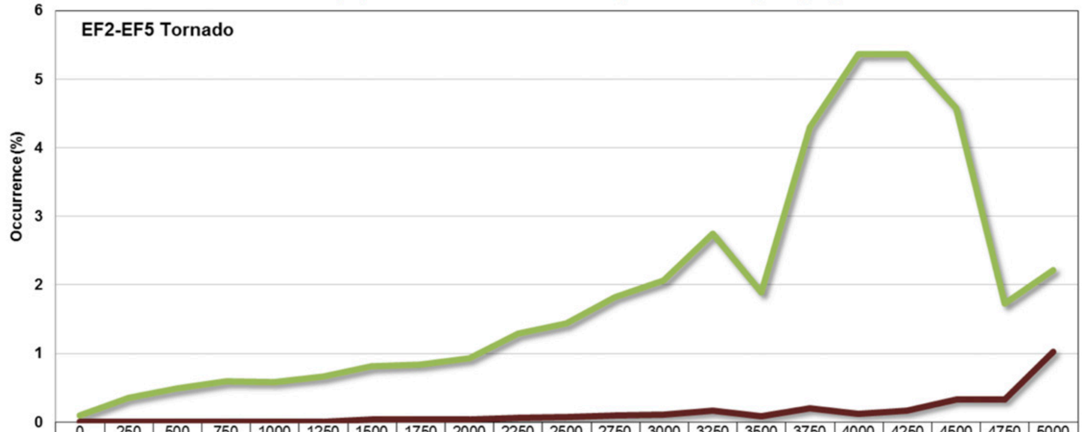

| | 0 | 250 | 500 | 750 | 1000 | 1250 | 1500 | 1750 | 2000 | 2250 | 2500 | 2750 | 3000 | 3250 | 3500 | 3750 | 4000 | 4250 | 4500 | 4750 | 5000 |
|---|---|---|---|---|---|---|---|---|---|---|---|---|---|---|---|---|---|---|---|---|---|
| 🟩 Nov-May (%) | 0.1 | 0.4 | 0.5 | 0.6 | 0.6 | 0.7 | 0.8 | 0.8 | 0.9 | 1.3 | 1.4 | 1.8 | 2.1 | 2.7 | 1.9 | 4.3 | 5.4 | 5.4 | 4.6 | 1.7 | 2.2 |
| 🟥 Jun-Oct (%) | 0.0 | 0.0 | 0.0 | 0.0 | 0.0 | 0.0 | 0.0 | 0.1 | 0.0 | 0.1 | 0.1 | 0.1 | 0.1 | 0.2 | 0.1 | 0.2 | 0.1 | 0.2 | 0.3 | 0.3 | 1.0 |
| Nov-May Events | 535 | 488 | 461 | 408 | 309 | 270 | 253 | 196 | 153 | 141 | 105 | 84 | 58 | 45 | 20 | 28 | 19 | 13 | 6 | 1 | 1 |
| Nov-May Environs | 540975 | 138222 | 95513 | 68953 | 52799 | 40976 | 31291 | 23303 | 16430 | 10959 | 7312 | 4597 | 2811 | 1637 | 1059 | 650 | 354 | 242 | 131 | 58 | 45 |
| Jun-Oct Events | 68 | 74 | 81 | 94 | 60 | 58 | 66 | 63 | 48 | 48 | 40 | 37 | 29 | 27 | 9 | 13 | 5 | 4 | 5 | 3 | 6 |
| Jun-Oct Environs | 691028 | 394388 | 329060 | 268780 | 220938 | 181389 | 149872 | 122243 | 96604 | 72645 | 52644 | 36527 | 24355 | 15849 | 10127 | 6233 | 3822 | 2349 | 1499 | 898 | 581 |

(b) 100mb Mixed-Layer CIN (J $kg^{-1}$)

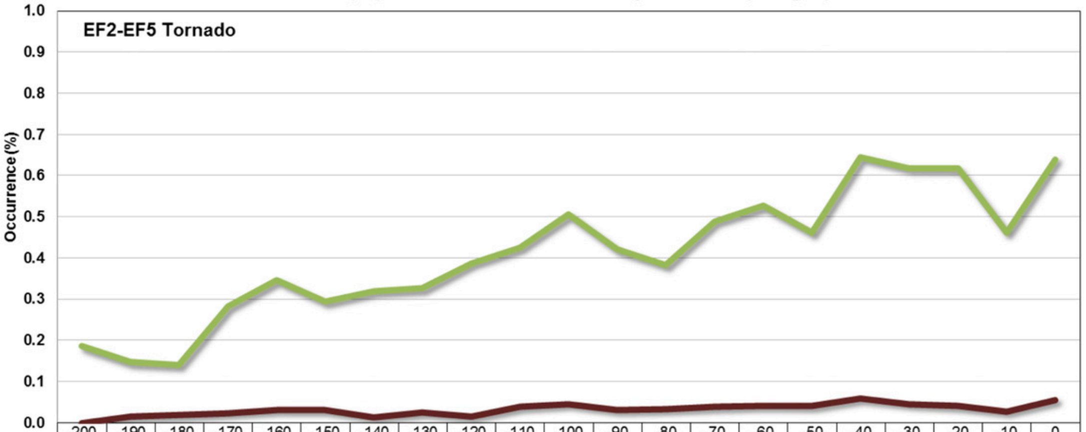

| | -200 | -190 | -180 | -170 | -160 | -150 | -140 | -130 | -120 | -110 | -100 | -90 | -80 | -70 | -60 | -50 | -40 | -30 | -20 | -10 | 0 |
|---|---|---|---|---|---|---|---|---|---|---|---|---|---|---|---|---|---|---|---|---|---|
| 🟩 Nov-May (%) | 0.2 | 0.1 | 0.1 | 0.3 | 0.3 | 0.3 | 0.3 | 0.3 | 0.4 | 0.4 | 0.5 | 0.4 | 0.4 | 0.5 | 0.5 | 0.5 | 0.6 | 0.6 | 0.6 | 0.5 | 0.6 |
| 🟥 Jun-Oct (%) | 0.0 | 0.0 | 0.0 | 0.0 | 0.0 | 0.0 | 0.0 | 0.0 | 0.0 | 0.0 | 0.0 | 0.0 | 0.0 | 0.0 | 0.0 | 0.0 | 0.1 | 0.0 | 0.0 | 0.0 | 0.1 |
| Nov-May Events | 14 | 12 | 13 | 28 | 39 | 37 | 44 | 50 | 66 | 80 | 108 | 101 | 105 | 155 | 190 | 194 | 328 | 391 | 518 | 790 | 146 |
| Nov-May Environs | 7583 | 8234 | 9293 | 9955 | 11254 | 12614 | 13773 | 15348 | 17038 | 18788 | 21346 | 24031 | 27449 | 31664 | 36081 | 42051 | 50814 | 63193 | 83881 | 171024 | 22816 |
| Jun-Oct Events | 0 | 4 | 5 | 7 | 10 | 11 | 6 | 11 | 8 | 21 | 28 | 22 | 27 | 36 | 46 | 53 | 94 | 96 | 121 | 194 | 33 |
| Jun-Oct Environs | 21063 | 22972 | 25359 | 27565 | 30703 | 34376 | 38062 | 41965 | 47402 | 53194 | 60251 | 68607 | 78466 | 91359 | 108344 | 128930 | 158471 | 205627 | 295043 | 676072 | 59883 |

FIG. 5. As in Fig. 4, but for (a) MLCAPE and (b) MLCIN.

SSCRAM system is used to study two separate, temporally continuous periods of significant tornado predictability using STP: higher predictability in N–M that includes the cool season and lower predictability in J–O that includes the warm season. In fact, J–O significant tornado conditional probabilities fall substantially, by a factor of generally around 5–10, from the corresponding N–M probabilities, and offer little to no variability among the ranges of STP values, as shown in Fig. 4. This approach suggests STP has limited forecast utility during J–O.

A major challenge exists in explaining the decrease in the utility of STP in forecasting significant tornadoes during J–O compared to N–M, as this notion is counterintuitive. This parameter lies at the forefront of diagnostic methods in assessing significant tornado potential, and the aforementioned findings suggest that significant tornado predictability falls during the transition from N–M to J–O. It is possible that this could be related to the greater predictability of more strongly forced convective events (e.g., Jankov and Gallus 2004) that are more characteristic of N–M than J–O. Furthermore, some of the N–M to J–O

(a) Effective Helicity ($m^2\ s^{-2}$)

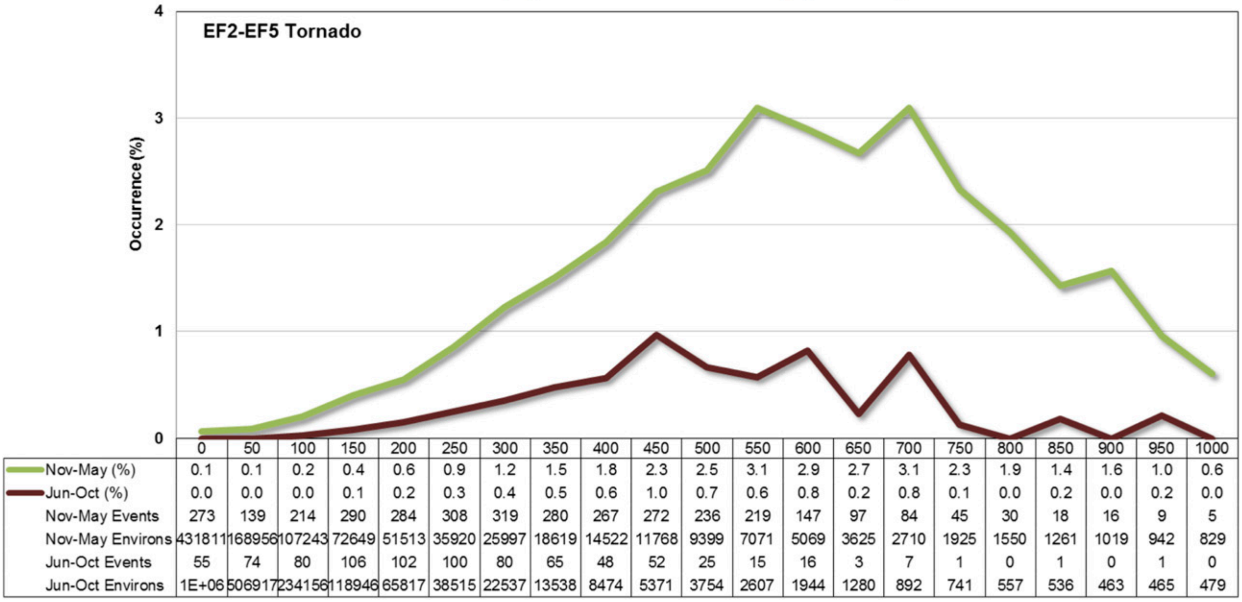

| | 0 | 50 | 100 | 150 | 200 | 250 | 300 | 350 | 400 | 450 | 500 | 550 | 600 | 650 | 700 | 750 | 800 | 850 | 900 | 950 | 1000 |
|---|---|---|---|---|---|---|---|---|---|---|---|---|---|---|---|---|---|---|---|---|---|
| 🟩 Nov-May (%) | 0.1 | 0.1 | 0.2 | 0.4 | 0.6 | 0.9 | 1.2 | 1.5 | 1.8 | 2.3 | 2.5 | 3.1 | 2.9 | 2.7 | 3.1 | 2.3 | 1.9 | 1.4 | 1.6 | 1.0 | 0.6 |
| 🟥 Jun-Oct (%) | 0.0 | 0.0 | 0.0 | 0.1 | 0.2 | 0.3 | 0.4 | 0.5 | 0.6 | 1.0 | 0.7 | 0.6 | 0.8 | 0.2 | 0.8 | 0.1 | 0.0 | 0.2 | 0.0 | 0.2 | 0.0 |
| Nov-May Events | 273 | 139 | 214 | 290 | 284 | 308 | 319 | 280 | 267 | 272 | 236 | 219 | 147 | 97 | 84 | 45 | 30 | 18 | 16 | 9 | 5 |
| Nov-May Environs | 431811 | 168956 | 107243 | 72649 | 51513 | 35920 | 25997 | 18619 | 14522 | 11768 | 9399 | 7071 | 5069 | 3625 | 2710 | 1925 | 1550 | 1261 | 1019 | 942 | 829 |
| Jun-Oct Events | 55 | 74 | 80 | 106 | 102 | 100 | 80 | 65 | 48 | 52 | 25 | 15 | 16 | 3 | 7 | 1 | 0 | 1 | 0 | 1 | 0 |
| Jun-Oct Environs | 1E+06 | 506917 | 234156 | 118946 | 65817 | 38515 | 22537 | 13538 | 8474 | 5371 | 3754 | 2607 | 1944 | 1280 | 892 | 741 | 557 | 536 | 463 | 465 | 479 |

(b) Effective Bulk Shear (kt)

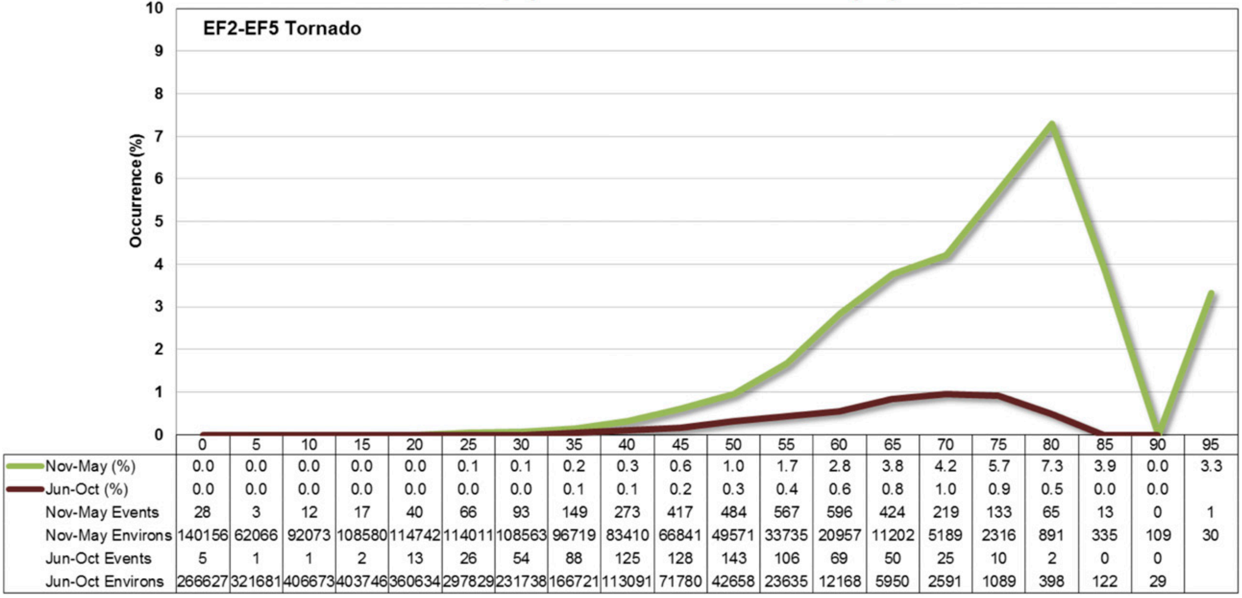

| | 0 | 5 | 10 | 15 | 20 | 25 | 30 | 35 | 40 | 45 | 50 | 55 | 60 | 65 | 70 | 75 | 80 | 85 | 90 | 95 |
|---|---|---|---|---|---|---|---|---|---|---|---|---|---|---|---|---|---|---|---|---|
| 🟩 Nov-May (%) | 0.0 | 0.0 | 0.0 | 0.0 | 0.0 | 0.1 | 0.1 | 0.2 | 0.3 | 0.6 | 1.0 | 1.7 | 2.8 | 3.8 | 4.2 | 5.7 | 7.3 | 3.9 | 0.0 | 3.3 |
| 🟥 Jun-Oct (%) | 0.0 | 0.0 | 0.0 | 0.0 | 0.0 | 0.0 | 0.0 | 0.1 | 0.1 | 0.2 | 0.3 | 0.4 | 0.6 | 0.8 | 1.0 | 0.9 | 0.5 | 0.0 | 0.0 | |
| Nov-May Events | 28 | 3 | 12 | 17 | 40 | 66 | 93 | 149 | 273 | 417 | 484 | 567 | 596 | 424 | 219 | 133 | 65 | 13 | 0 | 1 |
| Nov-May Environs | 140156 | 62066 | 92073 | 108580 | 114742 | 114011 | 108563 | 96719 | 83410 | 66841 | 49571 | 33735 | 20957 | 11202 | 5189 | 2316 | 891 | 335 | 109 | 30 |
| Jun-Oct Events | 5 | 1 | 1 | 2 | 13 | 26 | 54 | 88 | 125 | 128 | 143 | 106 | 69 | 50 | 25 | 10 | 2 | 0 | 0 | |
| Jun-Oct Environs | 266627 | 321681 | 406673 | 403746 | 360634 | 297829 | 231738 | 166721 | 113091 | 71780 | 42658 | 23635 | 12168 | 5950 | 2591 | 1089 | 398 | 122 | 29 | |

FIG. 6. As in Fig. 4, but for (a) effective SRH and (b) effective bulk shear.

decrease in the predictability of significant tornadoes using STP could be associated with the influence of the heterogeneities of mesoscale parameters and associated boundaries not resolved by the SSCRAM system on significant tornado potential, along with the lack of representation of advection processes influencing the downstream environment and other limitations of the SSCRAM system that Hart and Cohen (2016) address.

The reduction of forecast utility of STP from N–M to J–O is also reflected by the reduction of the predictability of significant tornadoes using individual components of the STP, as illustrated by Figs. 5 and 6. Figure 5 shows that the already limited predictability of MLCAPE in assessing significant tornado conditional probabilities is even more limited during J–O, transitioning from a weakly varying probability curve with increasing MLCAPE during N–M, to a near-flat curve with near-zero probabilities during J–O. The same general tendencies are evident for effective-layer storm-relative helicity, and effective bulk shear. While not

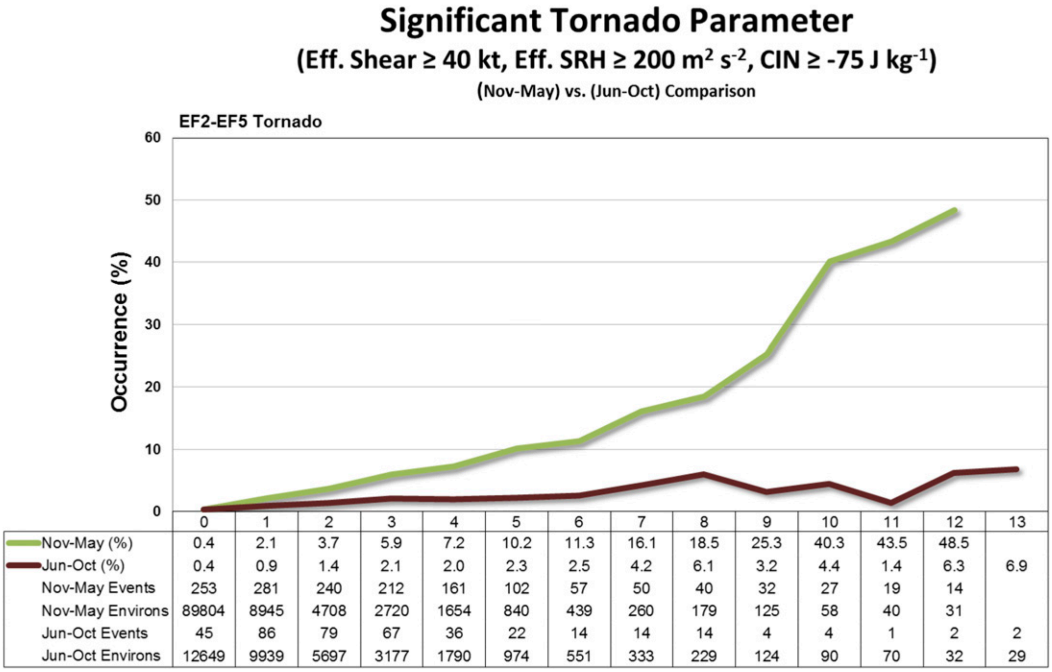

| | 0 | 1 | 2 | 3 | 4 | 5 | 6 | 7 | 8 | 9 | 10 | 11 | 12 | 13 |
|---|---|---|---|---|---|---|---|---|---|---|---|---|---|---|
| 🟩 Nov-May (%) | 0.4 | 2.1 | 3.7 | 5.9 | 7.2 | 10.2 | 11.3 | 16.1 | 18.5 | 25.3 | 40.3 | 43.5 | 48.5 | |
| 🟥 Jun-Oct (%) | 0.4 | 0.9 | 1.4 | 2.1 | 2.0 | 2.3 | 2.5 | 4.2 | 6.1 | 3.2 | 4.4 | 1.4 | 6.3 | 6.9 |
| Nov-May Events | 253 | 281 | 240 | 212 | 161 | 102 | 57 | 50 | 40 | 32 | 27 | 19 | 14 | |
| Nov-May Environs | 89804 | 8945 | 4708 | 2720 | 1654 | 840 | 439 | 260 | 179 | 125 | 58 | 40 | 31 | |
| Jun-Oct Events | 45 | 86 | 79 | 67 | 36 | 22 | 14 | 14 | 14 | 4 | 4 | 1 | 2 | 2 |
| Jun-Oct Environs | 12649 | 9939 | 5697 | 3177 | 1790 | 974 | 551 | 333 | 229 | 124 | 90 | 70 | 32 | 29 |

FIG. 7. As in Fig. 4, but using constraints of effective-layer SRH ≥ 200 $m^2 s^{-2}$, effective bulk shear magnitude ≥ 40 kt, and MLCIN ≥ −75 J $kg^{-1}$.

specifically analyzed by Hart and Cohen (2016) with respect to evaluating severe thunderstorm predictability, Fig. 5 also displays MLCIN, as Davies (2004) found that lower magnitudes of MLCIN correspond to higher frequencies of tornadoes rated F1–F4. We find that any modest signal for significant tornado probability to increase with decreasing magnitude of MLCIN during N–M largely vanishes during J–O. Figure 6 highlights the decline in the predictability of significant tornadoes using the kinematic parameters of effective SRH and effective bulk shear. Thus, Figs. 5 and 6 collectively demonstrate the decrease in the forecast utility of diagnostic variables in assessing significant tornado potential from N–M to J–O. These parameters summarize basic ingredients of severe thunderstorm environments and appear to offer little predictability in J–O. Even restricting to environmental cases of strong environmental shear [storm-relative helicity of over 200 $m^2 s^{-2}$, effective bulk shear over 40 kt (where 1 kt = 0.51 $m s^{-1}$), and weak CIN], which would further condition the dataset to focus on supercell thunderstorm potential, shows that STP offers substantially less utility for prediction in J–O compared to N–M (Fig. 7).

## 3. Discussion and conclusions

Parameters describing the kinematic and thermodynamic mesoscale environment of severe thunderstorms have become an important part of the process of assessing the likelihood for severe thunderstorm development in a short-term forecasting mode. Forecasters have relied on certain fields, such as CAPE and vertical shear, along with composite parameters like STP, to assess this environment from a diagnostic perspective. There may be utility in extending these diagnostic variables to express prognostic information, and such an undertaking is the purpose of SSCRAM (Hart and Cohen 2016). SSCRAM attempts to accomplish the challenge offered by Doswell and Schultz (2006) to garner prognostic power from diagnostic variables in a reproducible manner.

Hart and Cohen (2016) have demonstrated that it is certainly possible to quantitatively assign probabilities to severe thunderstorm hazard occurrence downstream of observed lightning occurrence, in general. Their results combine data through all months of the year. However, J–O offers a substantially more challenging forecast problem. Figure 8 provides an illustration of this problem through an individual J–O case, in which multiple supercell thunderstorms were ongoing over an area of relatively substantial values of significant tornado parameter (over 2) across parts of the lower Great Lakes and the Ohio valley region on 13 July 2015. None of these storms produced significant tornadoes. Yet, the only significant tornado of the day was well to the west, in south-central Kansas, in an environment

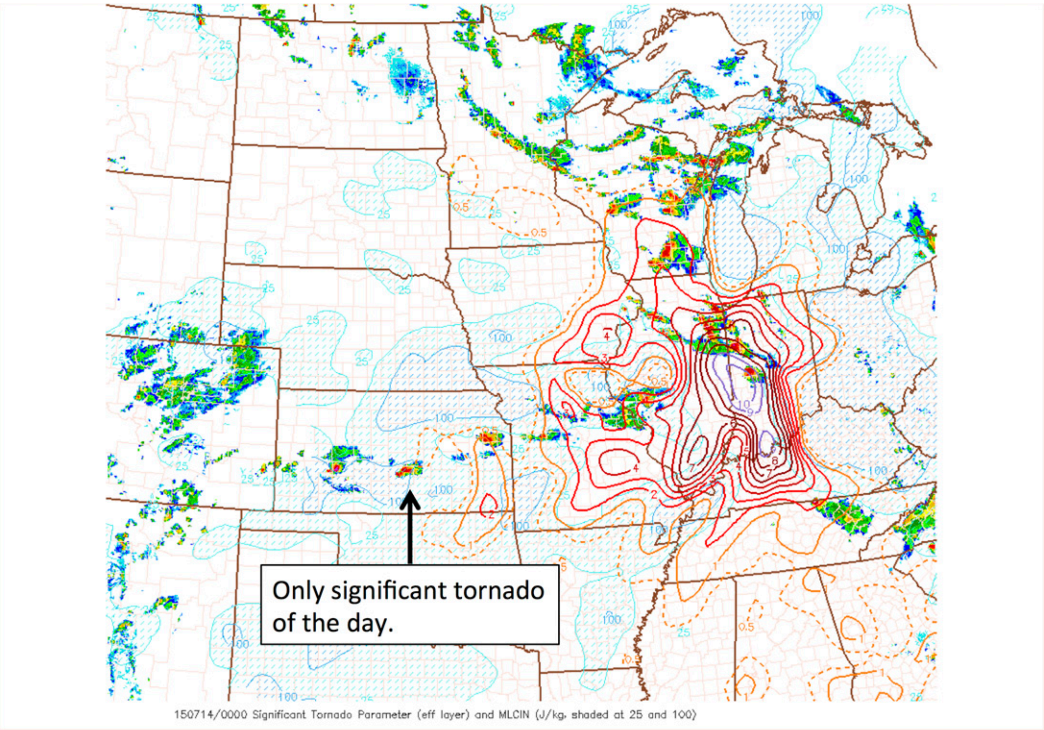

Only significant tornado of the day.

150714/0000 Significant Tornado Parameter (eff layer) and MLCIN (J/kg, shaded at 25 and 100)

FIG. 8. Overlay of significant tornado parameters (orange, red, and purple contours), MLCIN (light blue and darker blue contours with inner hatched areas), and mosaic radar imagery corresponding to the 0000 UTC Storm Prediction Center (SPC) mesoanalysis (Bothwell et al. 2002) graphics on 14 Jul 2015. The supercell thunderstorm that produced the only significant tornado of the day is marked in south-central KS.

characterized by substantially lower values of STP. This tornado was associated with a supercell thunderstorm evolving amid a background frontal zone.

We enumerate the number of grid boxes containing CG lightning combined with a constraint of STP being at least 3. This STP threshold is intended to identify environments that are strongly favorable for significant tornadoes. We find that 13 486 (11 445) grid boxes meet these constraints in N–M (J–O), while 1063 (211) grid boxes yield downstream significant tornadoes in N–M (J–O). As such, the exceedance probability of a significant tornado when STP values are at least 3 reduces from 7.9% in N–M to 1.8% in J–O. This is a dramatic reduction by over a factor of 4. The reduced efficiency of significant tornado environments from N–M to J–O, as identified using the SSCRAM system, is consistent with the reduced predictability of this phenomenon as previously discussed.

Ultimately, the SSCRAM technique suggests that significant tornadoes are less predictable during J–O compared to N–M. There are multiple possible explanations for the disparate probabilistic distributions shown in Figs. 2–7 for N–M versus J–O. First, one possible explanation is that cloud-to-ground (CG) lightning is not a good proxy for supercells (in the same STP environment) in J–O compared to N–M. The convective mode sample developed by Smith et al. (2012) suggests that supercells producing tornadoes or significant severe weather are less common in summer than spring, despite more numerous lightning grid hours in the summer. Likewise, the ratios of summer-to-spring grid-hour environments (within specific ranges of STP values in the presence of an observed supercell) are quite similar to the ratios of EF-scale damage class ratings for known tornadic supercells. However, the Smith et al. (2012) sample did not include supercells producing subsignificant hail or damaging winds, and it is conceivable that such supercells are more common in the summer versus the spring.

Another hypothesis is that the SSCRAM technique does not work as well during J–O owing to the possibility that the assumed storm motion procedure in SSCRAM is less applicable during this period. Yet another hypothesis is that the parameter components of STP are poor representations of significant tornado potential in J–O, when it is likely that STP lacks elements on the storm scale (e.g., surface boundary interactions) that might be important in the more isolated significant tornado events. Furthermore, the diminished predictability of significant tornadoes using STP during J–O may be related to limitations of the SSCRAM system. This includes unresolved heterogeneities of mesoscale parameters and related boundaries, unaccounted advection processes, and other limitations of the SSCRAM system addressed by Hart and Cohen (2016). The diminished predictability may also be attributable to a decrease in overall convective predictability from strongly forced regimes to weakly forced regimes and the much lower occurrence of events during J–O. While testing these hypotheses is outside of the scope of this paper, the SSCRAM technique has served to highlight the challenge of attempting to discern the predictability of significant tornadoes during the June–October time period, based on a robust database. These hypotheses could collectively provide the foundation for additional research related to improving significant tornado forecasting.

*Acknowledgments.* This work was completed at the Storm Prediction Center. The authors express deep gratitude for all of Richard Thompson's contributions to this work, including his thorough review of this paper, bettering its presentation and articulation of results in the broader context of significant tornado forecasting. The authors also thank Andy Dean of the SPC for his help in accumulating severe thunderstorm reports and associated mesoanalysis environmental data, Israel Jirak for many insightful comments used to improve this manuscript, as well as many staff members of the SPC for their engaging discussion regarding interpretation of the results presented in this study. The authors also greatly appreciate the feedback from three reviewers on this work: Matthew Bunkers of the National Weather Service Forecast Office in Rapid City, South Dakota, and two anonymous reviewers, all of whom provided reviews that greatly improved the quality of this manuscript.

## REFERENCES

Bothwell, P. D., J. A. Hart, and R. L. Thompson, 2002: An integrated three-dimensional objective analysis scheme in use at the Storm Prediction Center. Preprints, *21st Conf. on Severe Local Storms/19th Conf. on Weather Analysis and Forecasting/15th Conf. on Numerical Weather Prediction*, San Antonio, TX, Amer. Meteor. Soc., JP3.1. [Available online at https://ams.confex.com/ams/pdfpapers/47482.pdf.]

Bunkers, M. J., B. A. Klimowski, J. W. Zeitler, R. L. Thompson, and M. L. Weisman, 2000: Predicting supercell motion using a new hodograph technique. *Wea. Forecasting*, **15**, 61–79, doi:10.1175/1520-0434(2000)015<0061:PSMUAN>2.0.CO;2.

——, D. A. Barber, R. L. Thompson, R. Edwards, and J. Garner, 2014: Choosing a universal mean wind for supercell motion prediction. *J. Oper. Meteor.*, **2** (11), 115–129, doi:10.15191/nwajom.2014.0211.

Craven, J. P., and H. E. Brooks, 2004: Baseline climatology of sounding derived parameters associated with deep moist convection. *Natl. Wea. Dig.*, **28**, 13–24.

Darkow, G. L., 1968: The total energy environment of severe storms. *J. Appl. Meteor.*, **7**, 199–205, doi:10.1175/1520-0450(1968)007<0199:TTEEOS>2.0.CO;2.

——, 1969: An analysis of over sixty tornado proximity soundings. Preprints, *Sixth Conf. on Severe Local Storms*, Chicago, IL, Amer. Meteor. Soc., 218–221.

Davies, J. M., 2004: Estimations of CIN and LFC associated with tornadic and nontornadic supercells. *Wea. Forecasting*, **19**, 714–726, doi:10.1175/1520-0434(2004)019<0714:EOCALA>2.0.CO;2.

Doswell, C. A., III, 1987: The distinction between large-scale and mesoscale contribution to severe convection: A case study example. *Wea. Forecasting*, **2**, 3–16, doi:10.1175/1520-0434(1987)002<0003:TDBLSA>2.0.CO;2.

——, and D. M. Schultz, 2006: On the use of indices and parameters in forecasting severe storms. *Electron. J. Severe Storms Meteor.*, **1** (3). [Available online at http://www.ejssm.org/ojs/index.php/ejssm/issue/view/3.]

Edwards, R., A. R. Dean, R. L. Thompson, and B. T. Smith, 2012: Convective modes for significant severe thunderstorms in the contiguous United States. Part III: Tropical cyclone tornadoes. *Wea. Forecasting*, **27**, 1507–1519, doi:10.1175/WAF-D-11-00117.1.

Hart, J. A., and W. Korotky, 1991: The SHARP workstation v1.50 users guide. National Weather Service, 30 pp. [Available from NWS Eastern Region Headquarters, 630 Johnson Ave., Bohemia, NY 11716.]

——, and A. E. Cohen, 2016: The Statistical Severe Convective Risk Assessment Model. *Wea. Forecasting*, **31**, 1697–1714, doi:10.1175/WAF-D-16-0004.1.

Jankov, I., and W. A. Gallus Jr., 2004: MCS rainfall forecast accuracy as a function of large-scale forcing. *Wea. Forecasting*, **19**, 428–439, doi:10.1175/1520-0434(2004)019<0428:MRFAAA>2.0.CO;2.

Johns, R. H., and C. A. Doswell, 1992: Severe local storms forecasting. *Wea. Forecasting*, **7**, 588–612, doi:10.1175/1520-0434(1992)007<0588:SLSF>2.0.CO;2.

Maddox, R. A., 1976: An evaluation of tornado proximity wind and stability data. *Mon. Wea. Rev.*, **104**, 133–142, doi:10.1175/1520-0493(1976)104<0133:AEOTPW>2.0.CO;2.

Rasmussen, E. N., and R. B. Wilhelmson, 1983: Relationships between storm characteristics and 1200 GMT hodographs, low-level shear, and stability. Preprints, *13th Conf. on Severe Local Storms*, Tulsa, OK, Amer. Meteor. Soc., J5–J8.

Smith, B. T., R. L. Thompson, J. S. Grams, C. Broyles, and H. E. Brooks, 2012: Convective modes for significant severe thunderstorms in the contiguous United States. Part I: Storm classification and climatology. *Wea. Forecasting*, **27**, 1114–1135, doi:10.1175/WAF-D-11-00115.1.

——, ——, ——, and P. T. Marsh, 2015: Diagnosing the conditional probability of tornado damage rating using environmental and radar attributes. *Wea. Forecasting*, **30**, 914–932, doi:10.1175/WAF-D-14-00122.1.

Thompson, R. L., C. M. Mead, and R. Edwards, 2007: Effective storm-relative helicity and bulk shear in supercell thunderstorm environments. *Wea. Forecasting*, **22**, 102–115, doi:10.1175/WAF969.1.

——, B. T. Smith, J. S. Grams, A. R. Dean, and C. Broyles, 2012: Convective modes for significant severe thunderstorms in the contiguous United States. Part II: Supercell and QLCS tornado environments. *Wea. Forecasting*, **27**, 1136–1154, doi:10.1175/WAF-D-11-00116.1.

Togstad, W. E., J. M. Davies, S. J. Corfidi, D. R. Bright, and A. R. Dean, 2011: Conditional probability estimation for significant tornadoes based on Rapid Update Cycle (RUC) profiles. *Wea. Forecasting*, **26**, 729–743, doi:10.1175/2011WAF2222440.1.